Dielectric Susceptibility of Water in the Interface

Journal:	*The Journal of Physical Chemistry*
Manuscript ID	jp-2021-03720w.R1
Manuscript Type:	Perspective
Date Submitted by the Author:	n/a
Complete List of Authors:	Matyushov, Dmitry; Arizona State University, School of Molecular Sciences

Dielectric Susceptibility of Water in the Interface

Dmitry V. Matyushov*

School of Molecular Sciences and Department of Physics, Arizona State University, PO Box 871504, Tempe, AZ 85287-1504

E-mail: dmitrym@asu.edu

Abstract

It has long been anticipated that dielectric constants of polar liquids are reduced in the interfacial layer. Recent experiments and computer simulations support these expectations. A strong reduction of the dielectric constant is found in the direction perpendicular to a planar substrate, while the parallel response is bulk-like. This perspective highlights recent theoretical calculations and simulations with an eye on relating them to properties observable in the laboratory. The average interface dielectric constant computed from simulations connects to thin films experiments, but cannot be extended to screening of charges. In contrast to dielectric theories where a single dielectric constant gauges both the polarization energy and screening, these two signatures of dielectric polarization diverge on the molecular scale. The reduction of the dielectric constant of water in thin films is currently viewed as a combined effect of geometric confinement imposed by the substrate and the reconstruction of water hydrogen bonds in the surface layer.

Introduction

Understanding and characterization of interfaces remains a grand challenge for condensed matter science. Much of chemistry and all molecular biology belong to the realm of interfacial phenomena. In some cases heterogeneous systems can be analyzed as mixtures of well-characterized components. This is not the case with electrostatic interactions and electrically polarized interfaces. Because of the long-range character of Coulomb interactions, polarization of a mixture arises from a self-consistent solution inseparable into polarized components. This is known as Maxwell-Wagner polarization in theories of dielectrics.[1] Extending this view to microscopic and nanometer-scale interfaces of polar liquids and accounting for the specifics of the interfacial liquid structure turned out to be a challenging problem not only from the technical viewpoint, but equally so from the perspective of developing physically sound formulations producing observables accessible to laboratory measurements. The

latter aspect turned out to be particularly difficult to address with the recent proliferation of numerical simulations reporting highly detailed interfacial structures, which, nevertheless, are difficult to translate to observable properties. This perspective article highlights these difficulties and subtle nuances while keeping an eye on the need to develop physical theories and computational formalisms relating computations to the laboratory experiment. Following an account of recent theoretical and computational advances, a short overview of experimental results addressing electrically polarized interfaces is presented.

The dielectric susceptibility and the dielectric constant quantify the amount of energy stored in a polarized dielectric (a nonconducting material) and are expressed through capacitance in dielectric experiments. It is postulated that the dielectric constant is a material property, that is, it is specific to a given material and is independent of the sample shape.[2,3] This postulate, which is supported by empirical evidence, is central to all theories of dielectrics.[1] This is a nontrivial result since, due to the long-range character of Coulomb forces, the polarization of a dielectric sample depends on its shape. However, when all boundary conditions are correctly taken into account, the resulting dielectric constant is a material property.

Theories of dielectrics[1] use the postulate of the dielectric constant being a material property to calculate dielectric polarization for samples of simple geometry. A spherical region is typically separated from the macroscopic sample and characterized by the dipole moment $\mathbf{M}$ when the dielectric is polarized (see ref 3 for a formulation where this simplification is avoided). There is no macroscopic dipole in the absence of the field for paraelectric (in contrast to ferroelectric) materials. The dielectric constant is defined either through the macroscopic dipole induced in the material by the external field or by the variance of the macroscopic dipole, driven by thermal agitation, when the field is turned off (Kirkwood-Onsager equation, see below). Fluctuation relations can also be applied to specify polar response at the microscopic scale as discussed below.

Defining the dielectric constant in terms of the linear polarization of the sample (the

polarization route) requires yet another postulate of electrostatics of dielectrics. This is the postulate of locality of the Maxwell field $\mathbf{E}(\mathbf{r})$. The Maxwell field is the global (macroscopic) field characterizing the entire dielectric. It is defined as the statistical average of the sum of the electric field of external charges $\mathbf{E}_0(\mathbf{r})$ and the electric field of all molecular (bound) charges $\mathbf{E}_b(\mathbf{r})$. The assumption of locality means that the polarization density $\mathbf{P}(\mathbf{r})$ at some point $\mathbf{r}$ in the dielectric is proportional to the Maxwell field at the same point

$$\mathbf{P}(\mathbf{r}) = \epsilon_0 \chi \mathbf{E}(\mathbf{r}) = \epsilon_0(\epsilon - 1)\mathbf{E}(\mathbf{r}) \tag{1}$$

In this equation, χ is the dielectric susceptibility and ϵ is the dielectric constant; ϵ_0 is the vacuum permittivity.

The polarization density $\mathbf{P}$ in eq 1 is formally defined by connecting its divergence to the density ρ_b of the bound (molecular) charges

$$\rho_b = -\nabla \cdot \mathbf{P} \tag{2}$$

For water in the interface, ρ_b is calculated by adding atomic charges of protons and oxygens in a small volume and dividing the resulting charge by the volume. This is not a very practical recipe in many cases and one alternatively applies the multipolar expansion to represent $\mathbf{P}$ in terms of molecular multipoles.[4] The multipolar expansion leads to $\mathbf{P}$ given by a sum of the density of dipoles $\mathbf{P}_d$ and divergences of higher multipolar densities starting from the second-rank tensor field of the density of molecular quadrupoles $\mathbf{Q}$

$$\mathbf{P} = \mathbf{P}_d - \frac{1}{3}\nabla \cdot \mathbf{Q} + \ldots \tag{3}$$

The terms not shown here include the density of octupoles and of higher multipolar moments.[5]

The polarization density entering the macroscopic eq 1 is assumed to be averaged (in-

tegrated) over a small volume $\Omega(\mathbf{r})$ in the polarized dielectric. The divergence of $\mathbf{Q}(\mathbf{r})$ and of higher multipolar moments turns by integration into a surface integral over the surface of the volume element $\Omega(\mathbf{r})$. If this surface integral makes a vanishing contribution, one can associate $\mathbf{P}(\mathbf{r})$ with the density of the dipole moment in the chosen small volume $\mathbf{P}(\mathbf{r}) = \mathbf{P}_d(\mathbf{r}) = \mathbf{M}(\mathbf{r})/\Omega(\mathbf{r})$. The ability to follow these steps requires that the volume $\Omega(\mathbf{r})$ has a macroscopic dimension such that the dielectric constant ϵ remains a material property. This requirement is not fulfilled for polarization of microscopic interfaces, when the distances of interest are of the molecular length scale, and for polarization of liquids and solids around molecules.

In all problems related to polarization at the molecular scale, $\mathbf{P}(\mathbf{r})$ is not well defined since one cannot measure polarization density at a point. This problem might seem purely technical, but eq 1 carries a more fundamental problem related to the fact that the inhomogeneous Maxwell field $\mathbf{E}(\mathbf{r})$ cannot be measured either[6] (a fundamental difficulty realized already by Thompson[7]). The only parameter that has a physical meaning is the line integral of the Maxwell field, which represents the potential difference $\Delta\phi$ between two points

$$\Delta\phi = \int d\boldsymbol{\ell} \cdot \mathbf{E} \tag{4}$$

This restriction implies that the Maxwell field can be defined only when it can be viewed as constant between two reference points. To define the Maxwell field with microscopic precision, one has to measure the potential difference with the same precision. In most practical cases, it means that the Maxwell field has to be uniform to be well defined. This is the condition assumed in the dielectric experiment where the potential drop $\Delta\phi$ is applied between two plates of the plane capacitor separated by the distance d. The average Maxwell field is defined as $\langle E \rangle = \Delta\phi/d$. One has to stress that this definition does not preclude variations of the Maxwell field in the interfacial regions and, even in this simplified configuration, one

experimentally deals with the spatial average (Figure 1)

$$\langle E \rangle = \frac{\Delta\phi}{d} = \frac{1}{d}\int_0^d dz E \tag{5}$$

These arguments make clear that both vector fields, $\mathbf{P}(\mathbf{r})$ and $\mathbf{E}(\mathbf{r})$, are ill-defined on the microscopic length scale and in fact cannot be measured. One wonders if the scalar parameter ϵ connecting these ill-defined vector fields can still be associated with the material dielectric constant reported by the macroscopic dielectric experiment. This question applied to interfaces is the main topic of this article. Before turning to interfacial polarization, we want to quickly dwell on the limitations of eq 1 when applied to bulk dielectrics.

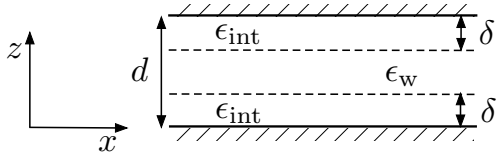

Figure 1: Diagram of the dielectric film viewed as a layered structure with interface dielectric constant ϵ_{int} in the interface of water with the capacitor plates and the bulk dielectric constant $\epsilon_w \simeq 80$ in the rest of the sample.

The assumption of locality of the polarization density and Maxwell fields is an approximation, as established by microscopic theories and computer simulations operating on the microscopic scale. When microscopic granularity of the material is involved, one has to replace the dielectric susceptibility χ in eq 1 with a second-rank tensorial function $\boldsymbol{\chi}(\mathbf{r}-\mathbf{r}')$ depending on the distance between two points in space $\mathbf{r}$ and $\mathbf{r}'$. Correspondingly, the local constitutive relation (eq 1) is replaced with the real-space convolution integral accounting for non-locality of the Maxwell field on the microscopic length scale of a few molecular diameters

$$\mathbf{P}(\mathbf{r}) = \epsilon_0 \int d\mathbf{r}' \boldsymbol{\chi}(\mathbf{r}-\mathbf{r}') \cdot \mathbf{E}(\mathbf{r}') \tag{6}$$

Physically, this equation implies that polarization at some point in space is not entirely defined by the Maxwell field at the same point, but instead by the Maxwell field in some

microscopic region in which dipoles of the material remain correlated. This result is usually cast in terms of the spatial Fourier transform allowing one to eliminate the real-space convolution and convert eq 6 into an algebraic equation, $\tilde{\mathbf{P}} = \epsilon_0 \tilde{\boldsymbol{\chi}} \cdot \tilde{\mathbf{E}}$, for the reciprocal-space fields indicated with tildes. This linear relation defines the k-dependent dielectric function $\tilde{\boldsymbol{\epsilon}}(k) = \mathbf{I} + \tilde{\boldsymbol{\chi}}(k)$, $I_{\alpha\beta} = \delta_{\alpha\beta}$. It is a second-rank tensor because the wavevector $\mathbf{k}$ introduces axial symmetry to the isotropic liquid. The axial second-rank tensor is defined by two scalar functions representing the response parallel to $\mathbf{k}$ (longitudinal, L) and perpendicular to $\mathbf{k}$ (transverse, T).[8] The two scalar components tend to the bulk dielectric constant ϵ at $k \to 0$.[9]

The reciprocal-space dielectric function has a well-defined physical meaning and has been calculated from liquid-state theories[10] and molecular dynamics simulations.[11] Nevertheless, its direct measurement by experiment has not been achieved so far. From the qualitative standpoint, $\tilde{\boldsymbol{\epsilon}}(k)$ describes the polar response at the length scale $\ell = 2\pi/k$ specified by the wavevector k. This physical meaning often invites analogies with the response of polar liquids in confinement. The connection is far from direct since $\tilde{\boldsymbol{\epsilon}}(k)$ does not incorporate two important effects significant to understanding the interfacial polar response: (i) the effect of geometric confinement, i.e., the reduction of the space available to the polar molecules to develop orientational correlations and (ii) physical orientational structure of interfaces. To illustrate the distinction between $\tilde{\boldsymbol{\epsilon}}(k)$ of bulk liquids from the dielectric response of interfaces, Figure 2 shows the transverse dielectric constant of SPC/E water calculated[12] from the dipolar transverse structure factor $S_T(k)$ replacing each molecular dipole with a point dipole

$$\tilde{\epsilon}_T(k) = 1 + 3yS_T(k) \tag{7}$$

where $y = \beta\rho m^2/(9\epsilon_0) \simeq 6.2$ for SPC/E water. One finds that this function starts with the bulk dielectric constant $\tilde{\epsilon}_T(0) = \epsilon_w \simeq 71$ at $k = 0$ and approaches the result for the ideal gas of dipoles $\epsilon_{\text{id}} = 1 + 3y \simeq 20$ when all dipolar correlations disappear at $k \to \infty$ ($\tilde{\boldsymbol{\epsilon}}(k)$ further decays at $k \to \infty$ when distributed intramolecular charge is taken into account[10]). The value ϵ_{id} is the lowest dielectric constant of bulk water considered as an ensemble of

dipoles. As discussed below, the dielectric constants in confinement and in interface are much lower, which requires specific antiparallel orientations of the neighboring dipoles (short-range correlations) reducing the Kirkwood factor below unity. This result comes in contrast to no dipolar correlations (either long-ranged or short-ranged) leading to $\epsilon_{\rm id}$.

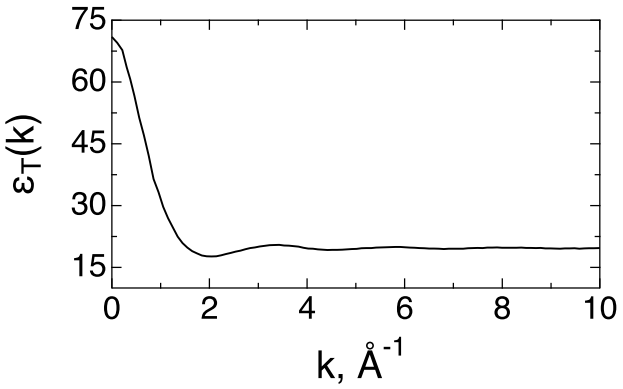

Figure 2: Transverse dielectric function $\tilde{\epsilon}_T(k)$ (eq 7) of bulk SPC/E water at 300 K[12] reaching the bulk value $\epsilon_w \simeq 71$ at $k = 0$ and the dielectric constant of an ideal gas of dipoles $\epsilon_{\rm id} = 1 + 3y$ at $k \to \infty$.

The transverse dielectric constant $\tilde{\epsilon}_T$ arises from the transverse susceptibility in reciprocal space $\tilde{\chi}_T(k) = \epsilon_0(\tilde{\epsilon}_T(k) - 1) = 3y\epsilon_0 S_T(k)$. This susceptibility and the longitudinal susceptibility $\tilde{\chi}_L(k) = \epsilon_0(1 - \tilde{\epsilon}_L(k)^{-1}) = 3y\epsilon_0 S_L(k)$ specify the free energy of spontaneous harmonic fluctuations of polarization density of a bulk polar liquid

$$F[\tilde{\mathbf{P}}] = \frac{1}{2}\sum_{\mathbf{k},a=L,T} \tilde{\chi}_a(k)^{-1}|\tilde{\mathbf{P}}_a(\mathbf{k})|^2 \tag{8}$$

The requirement of thermodynamic stability imposes the condition of positivity on both susceptibility functions: $\tilde{\chi}_a(k) > 0$, $a = \mathrm{L}, \mathrm{T}$. This conditions allows $\tilde{\epsilon}_L(k) < 0$ at intermediate wavevectors.[9] In contrast to singularities shown by $\tilde{\epsilon}_L(k)$, the longitudinal susceptibility is a positive and analytic function of the wavevector.

Quadratic, at small k, deviations of $\tilde{\chi}_a(k)$ from the macroscopic limit $k = 0$ determine

the exponential decay of polarization fluctuations $\delta\mathbf{P}_a(r)$ in direct space[13,14]

$$\langle \delta\mathbf{P}_a(r) \cdot \delta\mathbf{P}_a(0) \rangle \propto r^{-1} e^{-r/\Lambda_a} \tag{9}$$

where Λ_a is the correlation length. The longitudinal correlation length maintains its microscopic character: Λ_L tends to half of the molecular diameter $\sigma_s/2$ at $\epsilon \to \infty$. In contrast, $\Lambda_T \to \infty$ at $\epsilon \to \infty$.[13,14] The long-range character of dipolar correlations in polar liquids thus resides in the statistics of transverse polarization. However, solvation of spherical ions is given[15] in terms of the longitudinal susceptibility $\tilde{\chi}_L(k)$ and Λ_L enters the corresponding solvation energies.[14] This observation connects the problem of ion solvation to the problem of interfacial polarity. As we discuss below, it is the local longitudinal susceptibility that is mostly modified by the presence of the interface, while the transverse response is less affected.

The question of what is the length scale required to view the dielectric constant as a material property has fascinated the researchers for a long time. It has been anticipated that a slab of the dielectric should demonstrate a lower dielectric constant if the distance between the plates of the plane capacitor is reduced to a few molecular diameters.[16–18] For instance, the Stern and inner Helmholtz layers at the surface of a polarized metal electrode immersed in a polar liquid are often viewed as carrying a lower value of the dielectric constant.[5] As we discuss below, recent experiments[18] do not support this conjecture in regard to the diffuse layer. Nevertheless, to incorporate this suggestion, a position-dependent dielectric constant $\epsilon(\mathbf{r})$ is often introduced

$$\mathbf{P}(\mathbf{r}) = \epsilon_0(\epsilon(\mathbf{r}) - 1)\mathbf{E}(\mathbf{r}) \tag{10}$$

where the position $\mathbf{r}$ is used to label the distance from a substrate or a solute into the liquid solvent. One therefore anticipates $\epsilon(r) \to \epsilon$ at $r \to \infty$.

The previous discussion makes it clear that eq 10 combines three functions of the position in the interface neither of which can be measured in the laboratory experiment. One has to

look for an alternative to this unfortunate situation to be still able to characterize interfacial polarization. This alternative can be sought from measuring the electrostatic polarization free energy of a thin film sandwiched between two electrodes in a geometry similar to the plane capacitor of the conventional dielectric experiment. These types of measurements became possible with the development of atomic force microscopy (AFM) and, more specifically, through electrical force microscopy (EFM),[19] which combines the force measurement with the voltage applied between the cantilever tip and the substrate. Following earlier reports,[17,20,21] direct measurements have been recently reported for the dielectric constant of water in contact with a graphite substrate as a function of the water film thickness.[22] The dielectric constant in the direction perpendicular to the graphite plane was found to be as low as ~ 2 within the layer of water ~ 7 Å in thickness.

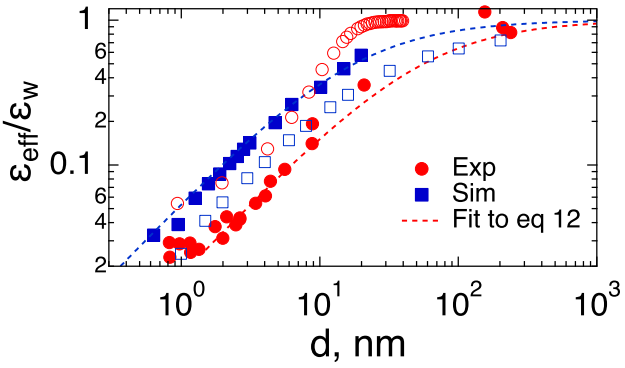

Figure 3: Dielectric constant ϵ_{eff} of the water layer vs thickness d. Experimental points (Exp) from ref[22] (red, filled circles) and from ref[17] (red, open circles) are shown without error bars. The dashed red line represents the fit of filled circles to eq 12 with $\epsilon_{\text{int}} = 2.1$ and $\delta = 0.74$ nm. Filled blue points (Sim) show the simulation results for SPC/E water[23] and the blue dashed line is the fit to eq 12 with $\epsilon_{\text{int}} = 2.3$ and $\delta = 0.29$ nm ($\epsilon_w = 71.2$ for SPC/E water). The open blue points refer to simulations of TIP3P water.[24] Adapted with permission from refs.[17,22–24] Copyright 2000 Elsevier, 2018 American Association for the Advancement of Science, and 2020 American Chemical Society.

The measurements of film capacitance are well described by the layered capacitor model (Figure 1) in which one assumes that the closest to the substrate layer with the thickness δ is described by the interface dielectric constant ϵ_{int} and the rest of the layer between two interfacial regions is assigned the bulk dielectric constant of water ϵ_{w}. The line integral in

eq 4 becomes

$$\Delta\phi = \int_0^d dz E_z(z) = D\left(\frac{2\delta}{\epsilon_{\rm int}} + \frac{d-2\delta}{\epsilon_{\rm w}}\right) \tag{11}$$

where the z-axis of the laboratory frame is directed perpendicular to the capacitor plates and D is the electric displacement specifying the density of free charges at the capacitor plates. Casting this equation in terms of the capacitance $C = \epsilon_0 A\epsilon_{\rm eff}/d$ (A is the electrode area), one obtains the effective dielectric constant depending on the film thickness d

$$\epsilon_{\rm eff}(d) = \left[\epsilon_{\rm w}^{-1} + (2\delta/d)\left(\epsilon_{\rm int}^{-1} - \epsilon_{\rm w}^{-1}\right)\right]^{-1} \approx \left[\epsilon_{\rm w}^{-1} + 2\delta/(\epsilon_{\rm int}d)\right]^{-1} \tag{12}$$

where in the last step $\epsilon_{\rm int} \ll \epsilon_{\rm w}$ has been used. The measurements thus effectively report the parameter $\delta/\epsilon_{\rm int}$. The value of the interface dielectric constant $\epsilon_{\rm int} \simeq 2.1$ was fixed by observing that the dielectric constant stops changing at $d < 1$ nm; the fit of the curve gives the thickness of the interfacial layer $\delta = 0.74$ nm (filled circles in Figure 3). Previous measurements[17] showed somewhat larger values $\epsilon_{\rm int} \simeq 4$ at $d \simeq 1$ nm (open circles in Figure 3). These data were extracted from fitting force-distance curves for the AFM tip placed at different separations from the mica substrate. Similar measurements employing the hydrophobic silicon substrate produced $\epsilon_{\rm int} \simeq 11$.[25]

To conclude this overview of the basic results of dielectric theories when applied to interfaces, it is important to note that many broadly accepted results of the theory of dielectrics have to change once the notion of the interface dielectric constant is adopted. As an illustrative example, one can turn to the textbook problem[1] of the dielectric sphere polarized by the external field (Figure 4). The standard formulation requires one to find the field inside the sphere polarized by the external field $E_0 = E_{0,z}$ directed along the z-axis of the laboratory frame. The depolarizing field is caused by the surface charge density $\sigma(\theta) = \sigma_1 \cos\theta$, where σ_1 refers to the expansion term in the first-order Legendre polynomial $P_1(\cos\theta) = \cos\theta$. The field inside the sphere is a sum of the external field and the field of the surface charge density

for which one can adopt $\sigma_1 = \epsilon_0(\epsilon_{\rm int} - 1)E$. The result of integration over the surface is

$$E = E_0 - \frac{\epsilon_{\rm int} - 1}{3} E \tag{13}$$

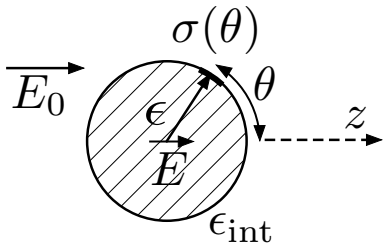

Figure 4: Polarization of the dielectric sphere by the field of external charges E_0. The spherical sample is characterized by the bulk dielectric constant ϵ and the interface dielectric constant $\epsilon_{\rm int}$

The dipole moment induced in the spherical sample with the volume V is found from the first-order perturbation theory in terms of the external field E_0. This leads to the following expression for the induced dipole

$$\frac{\langle M \rangle_E}{V} = \beta \frac{\langle M^2 \rangle}{V} E_0 = \epsilon_0(\epsilon - 1)E \tag{14}$$

where $\langle \dots \rangle_E$ refers to the statistical average in the presence of the external field and $\beta = (k_{\rm B}T)^{-1}$. In the case of a nonpolar liquid with molecular polarizability α, one adopts $\langle M \rangle_E = N\alpha E$ for N molecules in the volume V. For a more general case of a polar material, the account for eq 13 leads to the modified Clausius-Mossotti equation which turns to the standard form at $\epsilon_{\rm int} = \epsilon$

$$\frac{\epsilon - 1}{\epsilon_{\rm int} + 2} = \beta \frac{\langle \mathbf{M}^2 \rangle}{9\epsilon_0 V} \tag{15}$$

This modification is relevant for the dielectric response of confined water affected by a confining potential.[26] The surface-water interaction alters the structure of the surface layer, and the resulting dielectric constant of the sample depends on the surface-water potential.[27–29] We now turn to specifics of the analysis of numerical simulations aiming to calculate polar

response of interfacial water.

Theoretical formalisms

Computer simulations[23,30] of slabs of SPC/E water sandwiched between two graphene planes can be fitted to eq 12, but require a shorter saturation length δ of about one water diameter (blue filled squares and dashed line in Figure 3) compared to δ equal to two water diameters extracted from experiment.[22] Importantly, fitting simulations also requires a very small value of $\epsilon_{\rm int} \simeq 2$, although water is nonpolarizable in simulations and this result corresponds to a greater offset window between the interfacial dielectric constant and the limit of frozen response of molecular dipoles ($\epsilon_w = \epsilon_\infty$ for laboratory water and $\epsilon_w = 1$ for SPC/E water). Similar results were obtained for TIP3P water interacting with a single sheet of oxygen atoms modeling the substrate[24] (blue open squares in Figure 3). Overall, the slow saturation of $\epsilon_{\rm eff}(d)$ in Figure 3 does not reflect physical long-ranged correlations in the liquid, but, instead, represents the linear $\propto d$ scaling of the line integral in eq 11. Further, from the perspective of coarse-grained parameters describing polarization of the interface, there is little sense in defining a smooth function $\epsilon(z)$ interpolating between $\epsilon_{\rm int}$ and ϵ_w since such a function must change on a very short length scale and can hardly be measured. At present, a single interfacial parameter $\epsilon_{\rm int}$ seems to be a reasonable tradeoff between the need to parameterize the interfacial response and to avoid introducing concepts and parameters not accessible experimentally. It is also important to stress that $\epsilon_{\rm int}$ and ϵ carry very different meanings: while the former is an interface property sensitive to interactions with the substrate, the latter is a bulk material property. We now turn to computational approaches addressing the magnitude of $\epsilon_{\rm int}$.

The derivation in eq 11 shows that, similarly to the standard dielectric experiment, film measurements report the spatially averaged Maxwell field (eq 5). The measurements also indicate that the polarization of the film stops changing at $d \leq 2\delta$. One therefore can specify

the average polarization of the surface layer by taking the dipole moment induced by the field $\langle M(d)\rangle_E$ and dividing it by the layer volume dA

$$\langle P\rangle_E = \frac{\langle M(d)\rangle_E}{dA} = \epsilon_0\left(\epsilon_{\rm int}-1\right)E_{\rm int}, \quad d<2\delta \tag{16}$$

where $E_{\rm int}$ is the average Maxwell field $\langle E\rangle$ within the interface layer $d<2\delta$.

The association of the interface polarization with the interface dipole accumulated within a sufficiently thin layer offers a practical connection between laboratory measurements and analytical theories and numerical simulations. The average dipole moment of the microscopic layer can be calculated from configurations produced by computer simulations. Such statistical averages require strong electric fields to achieve sufficient sampling, which often drive the system out of the range of linear polarization.[31] A more practical approach, which does not require applying electric fields in the simulation protocol, is to use linear response. It connects the dipole induced by the field $\langle M(d)\rangle_E$ to statistical correlations computed on configurations in the absence of the external electric field. The recent surge of computational effort to address the problem of interfacial polarization has mostly followed this route. Still, an alternative approach, largely avoiding the need for extensive sampling, is to perform simulations at the conditions of a constant value of electric displacement[24,32] consistent with the dielectric experiment fixing the voltage on the capacitor plates.

The closest connection to eq 16 was realized in studies of the dielectric constant of water at the surface of a spherical solute polarizing water by a small probe charge q placed at its center.[33–35] The dipole moment of water is calculated in the radial shell with the radius $r=a+d$ composed of the solute radius a and water shell with the thickness d. Perturbation theory connects $\langle M(d)\rangle_E$ in eq 16 to the statistical correlation between fluctuations of the dipole moment of the radial water shell $\delta M(d)$ and the fluctuation of the electrostatic potential $\delta\phi_{\rm s}$ produced by water at the position of the probe charge. This correlation enters

the interface dielectric constant

$$\epsilon_{\rm int}^{-1} = 1 + \frac{\beta}{d}\langle \delta\phi_{\rm s}\delta M(d)\rangle \tag{17}$$

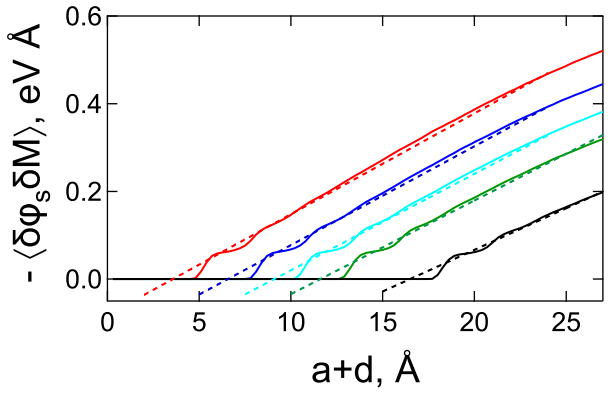

Figure 5: Calculation of the slope with the shell thickness for the cross-correlation of the shell dipole with the water electrostatic potential in eq 17. Each solid line corresponds to a solute with different size a in SPC/E water.[34] The dashed lines are linear fits used to determine the slope in eq 17. Reprinted with permission from ref.[34] Copyright 2016 American Institute of Physics.

The application of this algorithm is illustrated in Figure 5, where the radial projection of the shell dipole is calculated by summing up all radially projected molecular dipoles within the shell[34,36]

$$M(d) = \sum_{r_j<a+d} \hat{\mathbf{r}}_j \cdot \mathbf{m}_j, \quad \hat{\mathbf{r}}_j = \mathbf{r}_j/r_j \tag{18}$$

One can alternatively use the connection between the density of bound (molecular) charge ρ_b to the polarization density (eq 2) to determine the polarization of the radial shell

$$M(d) = -4\pi \int_0^d dr r^2 (d-r)\rho_b(r) \tag{19}$$

This equation goes beyond the dipolar approximation and incorporate higher multipoles in the shell polarization.[37]

The fluctuating dipole moment of the radial shell from either eq 18 or eq 19 is correlated in

eq 17 with the electrostatic potential at the position of the probe charge. The latter can be a physical or a fictitious charge. The calculations are performed for a neutral void in the latter case. Finally, the slope of the cross correlation is taken to arrive at $\epsilon_{\rm int}$. These calculations produced $\epsilon_{\rm int} \simeq 3-9$ at the surface of spherical nonpolar and charged solutes with the radii in the range 4–20 Å.[34] These numbers require an upward revision when corrected for finite-size effects.[38] The trend for $\epsilon_{\rm int}$ is to drop with increasing solute size (see below for a discussion), with the potential of reaching low values of $\epsilon_{\rm int}$ reported for flat surfaces (Figure 3).

Computer simulations provide parameters not accessible to laboratory measurements and allow one to calculate the instantaneous and statistically averaged values of the polarization density $\langle \mathbf{P} \rangle$ and of the microscopic electric field $\langle \mathbf{E}_{\rm mic} \rangle$. The latter, including both the external field and the field of molecular charges, can be associated with the Maxwell field of electrostatic theories. These two average fields can be combined to establish the position-dependent $\epsilon(\mathbf{r})$ from eq 10. As mentioned above, such calculations require applying significant external fields often driving the liquid out of equilibrium[23,31,39,40] and producing a reduction of the dielectric constant (nonlinear dielectric effect, $E_0 \geq 0.2$ V/Å for confined water[23,39]). An alternative, which is more often explored, is to use perturbation theories in terms of the perturbation caused by the field of external charges

$$H' = -\int d\mathbf{r} \mathbf{P}(\mathbf{r}) \cdot \mathbf{E}_0(\mathbf{r}) \tag{20}$$

The difficulty of this approach, which casts the averages in terms of $\mathbf{E}_0$, is that the dielectric constant is expressed as a linear response to the local Maxwell field (eq 1) instead of the external field. For a plane capacitor, $\langle E \rangle = \Delta\phi/d$ is fixed by the voltage at the plates, while E_0 is specified by the density of free charge carriers at the capacitor plates. The connection between the field of external charges and the Maxwell field depends on the sample shape and the resulting fluctuation relations require account of the geometry involved.[36] Here, we

discuss the microscopic, position-dependent dielectric constant for the most often considered slab geometry, when the equations are simplified by the fact that the electric field $\mathbf{E}_0$ is perpendicular to the slab. The field magnitude $E_0 = D/\epsilon_0$ is directly related to the electric displacement D.

Another significant advantage of the slab geometry is that the response measured perpendicular and parallel to the substrate give direct access to, correspondingly, longitudinal and transverse susceptibilities[8] defined from corresponding reciprocal-space functions at $k \to 0$ (Figure 2 and the discussion preceding eq 8). As mentioned above (eq 9), the longitudinal susceptibility is short-ranged and all long-range pathologies of dipolar interactions are contained in the transverse component. Given that experiments conducted so far have applied the external field perpendicular to the substrate, only longitudinal response has been accessed. Calculations of the interface dielectric constant at the surface of a spherical solute in eq 17 also provide access to the longitudinal response.

Applying the field perpendicular to the substrate, simulations resolve the position-dependent longitudinal response $\propto 1 - \epsilon_\perp(z)^{-1}$ and yield the position-dependent microscopic dielectric constant $\epsilon_\perp(z)$. When the field is applied parallel to the substrate plane, the transverse response $\propto \epsilon_\parallel(z) - 1$ is measured and leads to the parallel dielectric constant $\epsilon_\parallel(z)$. Computer simulations have shown that the response of interfacial water is highly anisotropic. The dielectric function becomes a second-rank axial tensor with parallel and perpendicular diagonal projections expressed through the fluctuation formulas[36,37,41]

$$\begin{aligned} \epsilon_\perp^{-1}(z) &= 1 - (\beta/\epsilon_0)\langle \delta P_z(z)\delta M_z\rangle, \\ \epsilon_\parallel(z) &= 1 + (\beta/\epsilon_0)\langle \delta P_x(z)\delta M_x\rangle \end{aligned} \tag{21}$$

where $\delta P_{x,z}$ and $\delta M_{x,z}$ specify deviations from the average values in the geometry shown in Figure 1. For simulations of periodically replicated slabs within a "tin-foil" boundary, the correlation function $\langle \delta P_z(z)\delta M_z\rangle$ needs to be divided by $1 + (\beta/\epsilon_0 V)\langle(\delta M_z)^2\rangle$ to account for polarization induced by images of the primary cell with the volume V.[42]

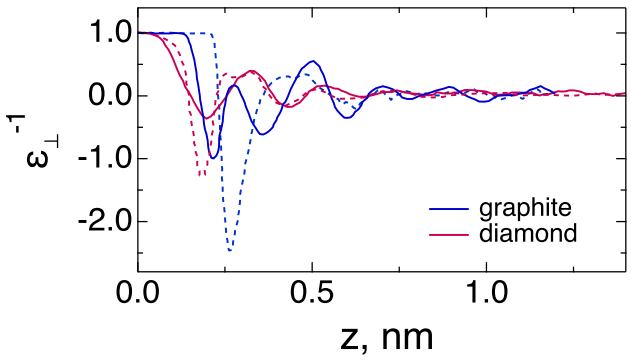

Figure 6: $\epsilon_{\perp}^{-1}(z)$ from MD simulations of water in contact with the hydrophilic diamond surface[37] (SPC/E water model, red) and with graphite (TIP4P/2005 water model, blue).[43] The solid lines indicate $P_z(z)$ calculated with the full multipolar expansion for water's bound charges and the dashed lines indicate the dipolar approximation for the polarization density. Adapted with permission from refs[37] and[43] Copyright 2011 American Physical Society and 2014 American Chemical Society.

Each projection defines the polar response of the interfacial water in a layer separated by the distance z from the substrate. The perpendicular dielectric modulus $\epsilon_{\perp}^{-1}(z)$ is a highly oscillatory function passing through multiple zeros[37,43,44] (Figure 6). Each zero of the dielectric modulus corresponds to a singularity of the perpendicular dielectric function.[44] An analog of this phenomenology for the k-dependent dielectric constant $\tilde{\epsilon}_L(k)$ is known as overscreening,[15] but it does not carry an equally clear meaning for the distant-dependent dielectric constant. What is common to these problems is that it is not the dielectric constant itself, but the longitudinal susceptibility $\propto 1 - \epsilon_{\perp}^{-1}$ that carries the physical meaning of the longitudinal polar response, and it is the susceptibility that is required to be positive to maintain thermodynamic stability (eq 8).

As mentioned above, the polarization density $P_z(z)$ of the successive layers can be calculated by assigning the dipole moment to each molecule within the layer or, more correctly, to include all molecular multipoles (mostly molecular quadrupole, but also the octupole[5]). The distinction between these two algorithms is indicated by the solid and dashed lines in Figure 6, where calculations[37,43] done for two different water models (SPC/E and TIP4P/2005) on two different substrates are reproduced. Molecular quadrupole is particularly important for

water and is less significant for other common polar liquids.

Despite the detailed microscopic information provided by $\epsilon_\alpha(z)$, $\alpha = \perp, \parallel$, it is also clear that neither the dielectric modulus $\epsilon_\perp^{-1}(z)$ nor the parallel dielectric constant $\epsilon_\parallel(z)$ are accessible experimentally as functions of z. A direct connection between these theoretical calculations and experimental measurements is achieved by noting that the perpendicular polarization density induced by the field, $P_E(z)$, is related to the longitudinal dielectric susceptibility[8]

$$P_E(z) = \epsilon_0 \left(1 - \epsilon_\perp^{-1}(z)\right) E_0 \tag{22}$$

The polarization of the sample with the thickness d in eq 16 is thus given in terms of the average dielectric modulus in the perpendicular projection[23,27,40,43–45]

$$\langle P \rangle_E = \epsilon_0 \left(1 - \langle \epsilon_\perp^{-1} \rangle\right) E_0 \tag{23}$$

where

$$\langle \epsilon_\perp^{-1} \rangle = \frac{1}{d} \int_0^d dz \epsilon_\perp^{-1}(z) \tag{24}$$

One also obtains from eq 16

$$\epsilon_{\text{int}}^{-1} = \langle \epsilon_\perp^{-1} \rangle. \tag{25}$$

This relation connects the formalism of the distant-dependent dielectric constant within the dielectric slab to the calculation of the average dipole within the d-shell in eq 17. However, it is clear that direct integration of $\epsilon_\perp^{-1}(z)$ is not practical given its irregular mathematical form (Figure 6) and one instead needs to produce $\epsilon_{\text{int}}^{-1}$ either from eq 17 or by using the standard fluctuation relation for the longitudinal susceptibility[8]

$$\epsilon_{\text{int}}^{-1} = \langle \epsilon_\perp^{-1} \rangle = 1 - (\beta/\Omega\epsilon_0)\langle (\delta M_z)^2 \rangle = 1 - 9yg_\perp \tag{26}$$

where Ω is the dielectric volume and $g_\perp$ is the perpendicular projection of the Kirkwood

factor. Note that eq 26 requires simulation of the liquid slab between two plane walls separated by the distance $d \leq 2\delta$.

Another difficulty of direct application of eq 24 lies in its high sensitivity[40] to the choice of the effective length d_{eff} required to reproduce the experimental data shown in Figure 3. The value of d (Figure 1) in the analysis of experiment[22] was chosen as $d \simeq L - 0.34$ nm to reflect dewetting of water interfacing a hydrophobic substrate and thus lowering the water thickness compared to the distance L between two substrate layers. A thin layer of strongly reduced water density was in fact found in recent simulations[24] where a three-layer capacitor model was used to fit the open squares in Figure 3. Instead of a single layer δ with ϵ_{int}, two layers with $\epsilon_1 \simeq 1.2$ and $\epsilon_2 \simeq 17.3$ were suggested. The decay of the interface dielectric constant with increasing radius of a spherical solute[34] might also be related to partial dewetting. The dielectric constant $\simeq 17$ of the actual interfacial layer turns out to be close to the value $\simeq 12 - 15$ calculated for SPC/E water at the surface of C_{60}[35] and with AFM measurements leading to $\epsilon_{\text{int}} \simeq 11$ on the hydrophobic substrate.[25]

The parallel dielectric constant $\epsilon_{\parallel}$ is typically found to be close to the bulk dielectric constant,[40] but it can fall above[46–49] or below[41,50] the bulk value depending on the system studied. A very significant increase of $\epsilon_{\parallel}$ (as high as ~ 700) over the bulk value was reported for water in carbon nanotubes.[46,48] A similarly large enhancement is reported for water confined between phospholipid planes.[40] Local density seems to play a major role in this enhancement. Similarly, the overall dipole moment variance $\langle(\delta\mathbf{M}(d))^2\rangle$ calculated within spherical shells around a spherical solute scales with the local density and is typically enhanced compared to the bulk.[51] Analogous scaling of the dielectric constant with density has been reported for carbon nanotubes[46] and for slit pores.[40,49] The situation with fluids confined in slabs and nanotubes is, however, more complex compared to local density profiles around solutes since one has to maintain equal chemical potentials between the bulk and confined components, and that requires altering the local density in confinement.[41]

Anisotropy of the dielectric constant must vanish when d approaches the macroscopic

limit. Either of two fluctuation relations in eq 21 can be used in this limit and one can define the average parallel projection in terms of the transverse dielectric susceptibility[8]

$$\epsilon_{\rm int} = \langle \epsilon_{\parallel} \rangle = 1 + (\beta/\Omega\epsilon_0)\langle (\delta M_x)^2 \rangle = 1 + 9yg_{\parallel} \tag{27}$$

where $g_{\parallel}$ is the parallel projection of the Kirkwood factor. Equations 26 and 27 can next be combined to obtain the variance of the total dipole moment of the sample $\langle (\delta \mathbf{M})^2 \rangle = \langle (\delta M_z)^2 \rangle + 2\langle (\delta M_x)^2 \rangle$. The scalar product is invariant to rotations of the laboratory frame and to the shape of the sample. This invariance is expressed by the Kirkwood-Onsager equation[1] for the bulk dielectric constant $\epsilon_{\rm int} \to \epsilon$

$$\frac{(\epsilon - 1)(2\epsilon + 1)}{9\epsilon} = \frac{\beta}{9\epsilon_0\Omega}\langle (\delta \mathbf{M})^2 \rangle = y\left(g_{\perp} + 2g_{\parallel}\right) \to yg_K \tag{28}$$

Two equations (eq 21) for the perpendicular and parallel dielectric projections hence can be combined into a single Kirkwood-Onsager equation for the bulk dielectric constant of a macroscopically large sample when the thickness of the slab grows to the macroscopic dimensions and interfacial anisotropy vanishes. Given that both $\langle (\delta \mathbf{M})^2 \rangle \propto N$ and $\Omega \propto N$ scale linearly with the number of particles N and the variance of the dipole moment does not depend on the sample shape, the dielectric constant becomes an intensive material property. Both simulations[23,27,28,30,52] and experiment[17,22] show that saturation to the macroscopic limit occurs on a large scale of $\sim$ 10 nm (Figure 3) reflecting the slow growth of the line integral in eq 11. The low value of $\epsilon_{\rm int}$ requires correspondingly low magnitudes of the Kirkwood correlation factor (eq 26). The value $g_{\perp} \simeq 0.2$ was calculated for dipolar projections perpendicular to the slab.[28,53] Since eq 26 requires $9yg_{\perp} < 1$, this result should be viewed as preliminary to characterize thin layers with $d < 2\delta$ (Figure 1). Nevertheless, negative correlations between orientations of the neighboring dipoles[44] must be present to allow low values of $\epsilon_{\rm int}$. This result comes is contrast to on average positive orientational correlations of dipoles in bulk laboratory water leading to the homogeneous Kirkwood factor estimated

as $g_K \simeq 2.6 - 2.8$.[54] Despite small $g_\perp$, water is not structurally frozen in the surface layer and its residence time is $\simeq$ 12 ps.[55] Further, small values of the Kirkwood factor due to preferential alignment are encountered also in bulk polar liquids: $g_K \simeq 0.62$ is found[56] due to preferential antiparallel alignment of acetonitrile molecules positioned equatorially to a tagged dipole.

In an attempt to connect the interface dielectric constant $\epsilon_{\rm int}$ to applications of electrostatics to molecular phenomena, one can turn to two classical problems of molecular electrostatics: (i) electrostatic solvation and (ii) screening of charges in polar dielectrics. Even for a macroscopic sample, the field created by a polarized dielectric in free space is specified by the interface dielectric constant[33] (Figure 4). One can view the free space as a void in the dielectric. This is the configuration directly related to electrostatic solvation. The electrostatic potential within a solute placed in a polar solvent is a sum of the potential of solute's free charges ϕ_0 and the potential of the surface charge at the dividing surface[57]

$$\phi(\mathbf{r}) = \phi_0(\mathbf{r}) + \phi_s(\mathbf{r}) = \phi_0(\mathbf{r}) + \oint_S d\mathbf{r}' \frac{\sigma(\mathbf{r}_S)}{4\pi\epsilon_0|\mathbf{r} - \mathbf{r}_S|} \tag{29}$$

The density $\sigma(\mathbf{r}_S)$ of the surface charge distributed over the dividing surface S is given as the polarization density $\langle P_n \rangle_E$ of the interface projected on the normal to the dividing surface and directed outward from the liquid.[4]

The solvent dielectric is obviously overall neutral and one wonders what is the physical meaning of the surface charge. It represents the effective force or electrostatic energy recorded in the void as produced by an inhomogeneous distribution of the interfacial dipoles (dipolar polarization density). Even though the overall charge is zero, the oriented ends of molecular dipoles located closer to the point of observation will contribute more to the electrostatic potential and the electrostatic force experienced by a probe charge placed inside the void. Simulations of cavities in water have shown that orientational preferences of interfacial water multipoles (both dipoles and quadrupoles) produce an overall positive potential inside the

cavity.[58,59] The effective surface charge density responsible for this cavity potential can be calculated from the fluctuation formula[33]

$$\sigma = -\beta\langle\delta P_n \delta E^C\rangle \tag{30}$$

where $\delta E^C = \sum_i q_i \delta\phi_{si}$ is the fluctuation of the Coulomb interaction energy of the solute charges q_i with the solvent. The free energy of electrostatic solvation ΔF_s is a sum of average electrostatic potentials $\langle\phi_{si}\rangle$ of the solvent at the positions of each solute charge q_i multiplied by those charges

$$\Delta F_s = \frac{1}{2}\sum_i q_i\langle\phi_{si}\rangle \tag{31}$$

In this framework, solvation thermodynamics is defined by the interface dielectric constant ϵ_{int}, reflecting the distribution of the surface charge, and not by the bulk dielectric constant ϵ. For solvation of a charge at the center of a spherical repulsive molecular core, this statement implies deviations from the Born model for ion solvation.

This definitive situation does not extend to screening of charges in polar liquids. The dielectric constant is defined above as the measure of the electrostatic free energy stored in the plane capacitor. The interface dielectric constant fits this definition, and it quantifies the electrostatic free energy stored in a plane capacitor only a few molecular diameters thick (the $2\times\delta$-layer, Figure 1). The bulk dielectric constant has an alternative meaning in theories of dielectrics to quantify the reduction of Coulomb interactions between charges in dielectrics compared to vacuum. One wonders if this definition extends to microscopic dimensions.

The interaction between charges in polarizable media is described by the potential of mean force (the free energy) equal to the reversible work to bring charges q_1 and q_2 from infinity to the distance d

$$U(d) = \frac{q_1 q_2}{4\pi\epsilon_0 d} + F_s(d) \tag{32}$$

The second term in this equation, which adds to the interaction energy of two charges in vacuum, is the reversible work of polarizing the dielectric. It can be calculated either by

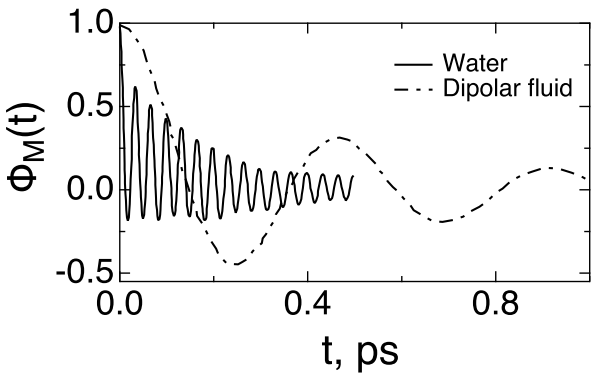

Figure 7: Normalized autocorrelation function of the dipole moment (eq 35) for SPC/E water[28] and Stockmayer dipolar fluid.[41] The thickness of the slab is 5 nm (water) and 1.7 nm (dipolar fluid). Adapted with permission from refs[41] and[28] Copyright 2007 and 2021 American Institute of Physics.

integrating the force over distance or from a fluctuation formula correlating the fluctuations of the solvent electrostatic potential $\delta\phi_{si}$ at two charges $(i = 1, 2)$[12,60]

$$F_s(d) = -\beta q_1 q_2 \langle \delta\phi_{s1} \delta\phi_{s2} \rangle \tag{33}$$

The bulk dielectric constant defines the $d \to \infty$ asymptote

$$F_s(d \to \infty) = -\frac{q_1 q_2}{4\pi\epsilon_0 d}\left(1 - \frac{1}{\epsilon}\right) \tag{34}$$

again displaying the longitudinal dielectric susceptibility[8] $\propto (1-\epsilon^{-1})$. However, at distances exceeding the closest approach by a few solvent diameters (2.87 Å for water), $F_s(d)$ becomes an oscillating function of d[61] and no simple relation to ϵ_{int} can be drawn. Oscillations of $F_s(d)$ are caused by overdamped collective excitations in the polar liquid (dipolarons[62]) appearing as singularities of the longitudinal susceptibility $1-\tilde{\epsilon}_L(k^*)^{-1}$ in the complex plane of wavevectors.[12] The complex part of the singularity k^*, $\tilde{\epsilon}_L(k^*, \omega) = 0$ is responsible for an exponential distance decay of dipolarons (eq 9) making them both spatially localized and exponentially decaying in time.[63] However, an oscillatory (underdamped) decay of the time

correlation functions for the perpendicular projection of the dipole moment

$$\Phi_M(t) = \langle M_z(t) M_z(0) \rangle / \langle M_z^2 \rangle \tag{35}$$

was found in simulations of water[28,39] and dipolar Stockmayer fluids[41] in slabs (Figure 7). These observations suggest a transition from an exponential temporal decay of dipolarons in bulk liquids to oscillatory, underdamped dynamics in confinement. This transition should display itself as a shift of k^* at which $\tilde{\epsilon}_L(k^*, \omega) = 0$ from the complex plane to the real axis where it should specify the dispersion $\omega(k^*)$ of dipolarons.

The screening part of the potential of mean force between two charges (eq 33) emerges as an infinite sum over all dipolaron excitations. Given many microscopic wavelengths involved, it is currently unclear if any connection can be drawn between the electrostatic energy stored in a thin film of a polar liquid and screening of Coulomb interactions between point charges at a similar length scale. A complex functional form of the potential of mean force at short distances suggests that no simple relation can be established between screening and a single scalar dielectric constant characterizing the interfacial layer. This was clearly demonstrated in recent simulations[64] in which the ion pair positioned normally to a graphene sheet in the water-graphene interface was flipped. The resulting Coulomb attraction between two ions turned out to be unequal in two configurations, thus precluding the use of a single scalar screening parameter.

The main result emerging from the comparison of the interface dielectric constant, used to quantify the free energy stored in a thin capacitor, with the screening of charges is that the latter problem requires a complex oscillatory potential of mean force at charge separation of the order of the molecular diameter and approaches asymptotically the standard result of dielectric theories at $d \to \infty$. As expected, the screening of charges in dielectrics is specified by the bulk dielectric constant ϵ at distances much exceeding the molecular diameter. This result connects to $\epsilon_{\text{eff}} \to \epsilon$ for macroscopic dielectric samples (eqs 12 and 28).

Nevertheless, solvation of charges within cavities created in liquids is determined by ϵ_{int}. Two different dielectric constants need to be used for problems of solvation and dielectric screening. Screening of charges at short distances in the interface cannot be reduced to a scalar parameter since it carries breaking of symmetry in respect to the ion exchange.[64]

Interpretation and experimental evidence

The experimental evidence[17,22,25] for a low value of the perpendicular dielectric constant within the water layer of $\delta \simeq 1$ nm has provoked several physical explanations. They mostly condense around the idea that the low value of the interface Kirkwood factor $g_\perp$ required to reach such a low interface dielectric constant can be related to the combined effect of geometric confinement by a low-dielectric medium, promoting antiparallel orientations, and a specific reconstruction of the hydrogen-bond network of water in the interface prohibiting dipolar fluctuations in the direction perpendicular to the substrate.

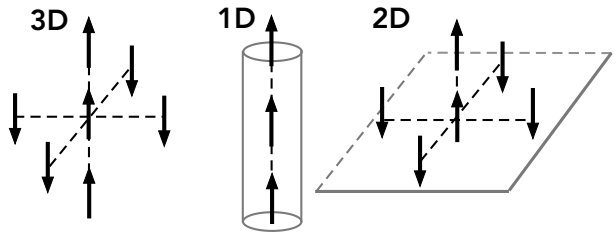

Figure 8: Cartoon of the preferential alignment of the neighboring dipoles in the bulk (3D), in a chain (1D), and on the surface of a substrate (2D). An octahedral first-shell coordination is used for illustration.

The idea that geometric confinement by a low-dielectric medium can shift the dielectric constant to either higher or lower values has merits (Figure 8). As a limiting case, a one-dimensional chain of dipoles ("1D" in Figure 8) has a significantly lower temperature of transition to the ferroelectric phase, when the dielectric constant diverges, than a three-dimensional dipolar liquid.[65] A single chain of water molecules thus arranges in a ferroelectric structure carrying a non-zero mean dipole moment.[66] The reason for a greater tendency of a dipolar chain to establish ferroelectric order is the elimination of equatorial dipoles, which

tend to orient antiparallel to a given tagged dipole in the bulk material ("3D" in Figure 8).[8] In contrast, the relative weight of equatorial antiparallel orientations is enhanced at the surface of a substrate when at least one dipole parallel to a tagged dipole is geometrically eliminated ("2D" in Figure 8). This picture was discussed in a recent study,[53] which notes "the dielectric constant reduction…is due to the dipolar field anisotropy and the replacement of water molecules with a nonpolarizable wall in a region where dipoles are positively correlated". The qualitative picture sketched in Figure 8 can be applied to the perpendicular projection of a tagged dipole and does not require the surface molecule to be oriented perpendicular to the substrate. Overall, experimental and theoretical results indicate that confinement by extended two-dimensional surfaces promotes locally antiparallel perpendicular dipolar projections leading to low values of $g_\perp$. In contrast to $g_\perp$, the Kirkwood factor $g_K = (S_L(0) + 2S_T(0))/3$ is the trace[14] including both the longitudinal, $S_L(0)$, and transverse, $S_T(0)$ (eq 7), structure factors in the macroscopic limit $k \to 0$ (see arguments leading to eq 28). Even when calculated as a function of the cutoff distance,[53] g_K does not provide access to the longitudinal response. From this perspective, it is incorrect[67] to apply the Kirkwood-Onsager equation to calculate $\epsilon_\perp(z)$.[53,68]

Measurements of polarization in response to static fields cannot distinguish between the generic effect of geometric confinement and a more specific contribution of interfacial hydrogen bonds. A computational report of a low ϵ_{int} for a broad list of polar liquids[23] offers support to the former scenario. The two scenarios can be distinguished experimentally by measuring perpendicular polarization at frequencies exceeding typical frequencies of molecular rotations. This goal was achieved in recent experiments where localized surface plasmons probed the perpendicular projection of water's refractive index in slabs with confinement gaps ranging from 10 nm to 80 nm.[69] Given that water molecules are nearly isotropically polarizable, the outcome of these measurements should not be affected by orientational restrictions imposed by interfacial hydrogen bonds. A substantial reduction of the refractive index suggests that mere confinement is behind the reduction of the dielectric response.[53]

The refractive index is further reduced by switching from a hydrophilic to a hydrophobic substrate, which must reflect a reduction of the interfacial density at a hydrophobic surface, which is also in line with the recent computational finding of a small gap between water and a model hydrophobic substrate.[24]

Even though measurements of the refractive index support the picture of geometric confinement as the primary origin of the dielectric constant reduction, one cannot completely disregard the notion that interfacial water is more structured than bulk water. This is supported by the appearance of the ice peak in the O-H stretch region recorded in the sum-frequency generation (SFG) spectrum.[70] A more subtle picture also comes from simulations which show that ϵ_{int} changes for water at the surface of fullerenes carrying different charges.[35] The change is caused by a structural transition of interfacial water connected to the release of dangling O-H bonds:[71] ϵ_{int} passes through a peak at the transition point. These results suggest that the network of hydrogen bonds in the interface contributes to the low value of ϵ_{int}, although it is likely not the main contributor to the reduction of ϵ_{int} relative to ϵ. The crossover from in-plane orientations of interfacial waters, typical for hydrophobic solvation,[72] to a large population of dangling O-H bonds was recorded by X-ray absorption of water on gold substates under a negative bias.[73] The effect of the substrate bias on ϵ_{int} is therefore testifiable experimentally, for instance by fitting the force-distance curves produced by AFM.[17,25] Addition of methanol[70] and other surfactants[74] to water was shown to quench dangling O-H bonds and to strongly modify the force between an air bubble and the AFM tip.[21] Given the effect of O-H dangling bonds on ϵ_{int},[35] this observation offers an additional experimental parameter to vary in studies of interfacial dielectric constant.

The reduction of the local density at a hydrophobic substrate should allow a stronger network of hydrogen bonds. Water under varying pressure effectively behaves as a mixture of high-density and low-density components. Increasing pressure breaks hydrogen bonds converting water to a predominantly high-density, fragile liquid,[75] which is anticipated to carry properties of many closely-packed polar liquids. An opposite effect of density expan-

sion at a hydrophobic substrate should promote stronger hydrogen bonds and constrain the perpendicular polar response. Therefore, if the picture of hydrogen bond restructuring to affect $\epsilon_{\rm int}$ in addition to geometric confinement is correct, one can anticipate an increase of $\epsilon_{\rm int}$ when pressure is elevated in the bulk. The temperature dependence $\epsilon_{\rm int}(T)$ serves as an additional indicator of an enhanced structure of interfacial water: the logarithmic derivative $\partial \ln \epsilon / \partial \ln T$ is $\simeq -1.37$ for bulk water ($\simeq -1.14$ for SPC/E water[76]), while the same derivative for SPC/E water at the surface of a charged C_{60}^{-3} is only -0.37 at $T = 300$ K.[35]

As mentioned above, screening of Coulomb interactions between free charge carriers is not directly related to $\epsilon_{\rm int}$, but still reflects the specifics of the interface in which screening occurs.[40,64] The electrostatic potential created by the interface at a substrate can be inferred from second harmonic generation (SHG) spectroscopy.[77] The third-order polarization of the interface is the product of electric fields E_ω of two incident photons and the static interfacial electric field. Integration of this polarization through the interfacial region results in the contribution equal to $\chi^{(3)} E_\omega E_\omega \langle \phi_s \rangle$ to the second-order polarization. Here, $\chi^{(3)}$ is the third-order nonlinear susceptibility and $\langle \phi_s \rangle$ is the average surface potential produced by the medium. It mostly comes from electrolyte ions and, at sufficiently small ionic concentrations (< 10 mM), the variation of the SHG signal with the electrolyte concentration allows access to an effective dielectric constant responsible for charge screening.[18] It was found that the dielectric constant representing screening of charges within the Debye screening length is well represented by the bulk value. This conclusion is in line with theoretical arguments requiring different dielectric constants for describing screening of charges and polarization of the interfacial layer.

Conclusions

An overview of theoretical methods presented here is meant to show that one can consistently define the dielectric constant of a thin interfacial layer and connect this definition to the

laboratory experiment measuring the capacitance of a thin film. The general outcome of both theoretical and experimental studies is that all polar liquids (protic and nonprotic) demonstrate a reduced perpendicular dielectric constant in the interface. This general result is likely related to the effect of geometric confinement promoting antiparallel orientations of the interfacial dipoles (Figure 8). Water shows a wider interfacial region of reduced polarity compared to other polar liquids because of energetic preferences of interfacial hydrogen bonds extending surface-induced perturbation further into the bulk. It appears that the hydrogen-bond network in the first surface layer of water amplifies the general trend found for all polar liquids by stabilizing in-plane orientations of water molecules. The convergence to the bulk limit with increasing slab thickness is therefore slower for water than for nonprotic liquids.[27]

One is nevertheless warned not to blindly extend the dielectric response in thin films to screening of charges in the interface. The interfacial dielectric constant quantifies the ability of the liquid layer to polarize and store electrostatic free energy, while screening quantifies the reduction of Coulomb interactions by polarized dipoles. In contrast to dielectric theories for which a single dielectric constant is used to gauge both the polarization energy and screening, these two properties of dielectric polarization diverge on the molecular scale and, potentially, even on the mesoscale. Electrostatic solvation of molecules is described by the interface dielectric constant, an interfacial property, but screening of charges cannot be described by a single scalar parameter characterizing the interfacial polar response.

Acknowledgement

This research was supported by the National Science Foundation (CHE-1800243).

References

(1) Scaife, B. K. P. *Principles of Dielectrics*; Clarendon Press: Oxford, 1998.

(2) Ramshaw, J. D. Exsistence of the dielectric constant in regid-dipole fluids: The direct correlation function. *J. Chem. Phys.* **1972**, *57*, 2684.

(3) Høye, J. S.; Stell, G. Statistical mechanics of polar systems. *J. Chem. Phys.* **1976**, *64*, 1952.

(4) Jackson, J. D. *Classical Electrodynamics*; Wiley: New York, 1999.

(5) Bonthuis, D. J.; Gekle, S.; Netz, R. R. Profile of the static permittivity tensor of water at interfaces: Consequences for capacitance, hydration interaction and ion adsorption. *Langmuir* **2012**, *28*, 7679–7694.

(6) Pao, Y. H. In *Mechanics Today*; Nemat-Nasser, S., Ed.; Pergamon Press Inc.: Oxford, UK, 1978; pp 209–305.

(7) Thompson Lord Kelvin, W. *Reprint of Papers on Electrostatics and Magnetism*, 2nd ed.; MacMillan and Co.: London, 1884, sec 479.

(8) Madden, P.; Kivelson, D. A consistent molecular treatment of dielectric phenomena. *Adv. Chem. Phys.* **1984**, *56*, 467–566.

(9) Dolgov, O. V.; Kirzhnits, D. A.; Maksimov, E. G. On an admissible sign of the static dielectric function of matter. *Rev. Mod. Phys.* **1981**, *53*, 81–93.

(10) Raineri, F. O.; Resat, H.; Friedman, H. L. Static longitudinal dielectric function of model molecular fluids. *J. Chem. Phys.* **1992**, *96*, 3068.

(11) Fonseca, T.; Ladanyi, B. M. Wave vector dependent static dielectric properties of associated liquids: Methanol. *J. Chem. Phys.* **1990**, *93*, 8148–8155.

(12) Seyedi, S.; Martin, D. R.; Matyushov, D. V. Screening of Coulomb interactions in liquid dielectrics. *J. Phys.: Condense Matter* **2019**, *31*, 325101.

(13) Wertheim, M. S. Exact solution of the mean spherical model for fluids of hard spheres with permanent electric dipole moments. *J. Chem. Phys.* **1971**, *55*, 4291–4298.

(14) Matyushov, D. V. Solvent reorganization energy of electron transfer in polar solvents. *J. Chem. Phys.* **2004**, *120*, 7532–7556.

(15) Kornyshev, A. A.; Sutmann, G. The shape of the nonlocal dielectric function of polar liquids and the implications for thermodynamic properties of electrolytes: A comparative study. *J. Chem. Phys.* **1996**, *104*, 1524.

(16) Debye, P.; Pauling, L. The inter-ionic attraction theory of ionized solutes. IV. The influence of variation of dielectric constant on the limiting law for small concentrations. *J. Am. Chem. Soc.* **1925**, *47*, 2129–2134.

(17) Teschke, O.; Ceotto, G.; De Souza, E. F. Interfacial aqueous solutions dielectric constant measurements using atomic force microscopy. *Chem. Phys. Lett.* **2000**, *326*, 328–334.

(18) Boamah, M. D.; Ohno, P. E.; Geiger, F. M.; Eisenthal, K. B. Relative permittivity in the electrical double layer from nonlinear optics. *J. Chem. Phys.* **2018**, *148*, 222808.

(19) Butt, H. J. Electrostatic interaction in atomic force microscopy. *Biophys. J.* **1991**, *60*, 777–785.

(20) Teschke, O.; Ceotto, G.; de Souza, E. F. Interfacial water dielectric-permittivity-profile measurements using atomic force microscopy. *Phys. Rev. E* **2001**, *64*, 011605.

(21) Teschke, O.; de Souza, E. F. Water molecule clusters measured at water/air interfaces using atomic force microscopy. *Phys. Chem. Chem. Phys.* **2005**, *7*, 3856–3865.

(22) Fumagalli, L.; Esfandiar, A.; Fabregas, R.; Hu, S.; Ares, P.; Janardanan, A.; Yang, Q.; Radha, B.; Taniguchi, T.; Watanabe, K. et al. Anomalously low dielectric constant of confined water. *Science* **2018**, *360*, 1339–1342.

(23) Motevaselian, M. H.; Aluru, N. R. Universal reduction in dielectric response of confined fluids. *ACS Nano* **2020**, *14*, 12761–12770.

(24) Deißenbeck, F.; Freysoldt, C.; Todorova, M.; Neugebauer, J.; Wippermann, S. Dielectric properties of nano-confined water: a canonical thermopotentiostat approach. *Phys. Rev. Lett.* **2021**, *126*, 136803.

(25) Teschke, O.; De Souza, E. F. Electrostatic response of hydrophobic surface measured by atomic force microscopy. *Appl. Phys.Lett.* **2003**, *82*, 1126–1128.

(26) Muñoz-Santiburcio, D.; Marx, D. Confinement-controlled aqueous chemistry within nanometric slit pores. *Chem. Rev.* **2021**, *121*, 6293–6320.

(27) Mondal, S.; Acharya, S.; Bagchi, B. Altered polar character of nanoconfined liquid water. *Phys. Rev. Res.* **2019**, *1*, 033145.

(28) Mondal, S.; Bagchi, B. Anomalous dielectric response of nanoconfined water. *J. Chem. Phys.* **2021**, *154*, 044501.

(29) Ruiz-Barragan, S.; Muñoz-Santiburcio, D.; Körning, S.; Marx, D. Quantifying anisotropic dielectric response properties of nanoconfined water within graphene slit pores. *Phys. Chem. Chem. Phys.* **2020**, *22*, 10833–10837.

(30) Zhang, C. Note: On the dielectric constant of nanoconfined water. *J. Chem. Phys.* **2018**, *148*, 156101.

(31) Yeh, I.-C.; Berkowitz, M. L. Dielectric constant of water at high electric fields: Molecular dynamics study. *J. Chem. Phys.* **1999**, *110*, 7935–7942.

(32) Zhang, C.; Sprik, M. Computing the dielectric constant of liquid water at constant dielectric displacement. *Phys. Rev. B* **2016**, *93*, 144201.

(33) Matyushov, D. V. Electrostatics of liquid interfaces. *J. Chem. Phys.* **2014**, *140*, 224506.

(34) Dinpajooh, M.; Matyushov, D. V. Dielectric constant of water in the interface. *J. Chem. Phys.* **2016**, *145*, 014504.

(35) Sarhangi, S. M.; Waskasi, M. M.; Hashemianzadeh, S. M.; Matyushov, D. Effective dielectric constant of water at the interface with charged C_{60} fullerenes. *J. Phys. Chem. B* **2019**, *123*, 3135–3143.

(36) Ballenegger, V.; Hansen, J.-P. Dielectric permittivity profiles of confined polar liquids. *J. Chem. Phys.* **2005**, *122*, 114711.

(37) Bonthuis, D. J.; Gekle, S.; Netz, R. R. Dielectric profile of interfacial water and its effect on double-layer capacitance. *Phys. Rev. Lett.* **2011**, *107*, 166102.

(38) Dinpajooh, M.; Matyushov, D. V. Dielectric constant at the surface of a spherical solute: Ewald sum corrections. *J. Phys. Chem. B* submitted.

(39) De Luca, S.; Kannam, S. K.; Todd, B. D.; Frascoli, F.; Hansen, J. S.; Daivis, P. J. Effects of confinement on the dielectric response of water extends up to mesoscale dimensions. *Langmuir* **2016**, *32*, 4765–4773.

(40) Loche, P.; Ayaz, C.; Wolde-Kidan, A.; Schlaich, A.; Netz, R. R. Universal and nonuniversal aspects of electrostatics in aqueous nanoconfinement. *J. Phys. Chem. B* **2020**, *124*, 4365–4371.

(41) Froltsov, V. A.; Klapp, S. H. L. Dielectric response of polar liquids in narrow slit pores. *J. Chem.Phys.* **2007**, *126*, 114703.

(42) Stern, H. A.; Feller, S. E. Calculation of the dielectric permittivity profile for a nonuniform system: Application to a lipid bilayer simulation. *J. Chem. Phys.* **2003**, *118*, 3401–3412.

(43) Parez, S.; Předota, M.; Machesky, M. Dielectric properties of water at rutile and

graphite surfaces: Effect of molecular structure. *J. Phys. Chem. C* **2014**, *118*, 4818–4834.

(44) Schlaich, A.; Knapp, E. W.; Netz, R. R. Water dielectric effects in planar confinement. *Phys. Rev. Lett.* **2016**, *117*, 048001.

(45) Jalali, H.; Ghorbanfekr, H.; Hamid, I.; Neek-Amal, M.; Rashidi, R.; Peeters, F. M. Out-of-plane permittivity of confined water. *Phys. Rev. E* **2020**, *102*, 022803.

(46) Renou, R.; Szymczyk, A.; Maurin, G.; Malfreyt, P.; Ghoufi, A. Superpermittivity of nanoconfined water. *J. Chem. Phys.* **2015**, *142*, 184706.

(47) Mondal, S.; Bagchi, B. Water in carbon nanotubes: Pronounced anisotropy in dielectric dispersion and its microscopic origin. *J. Phys. Chem. Lett.* **2019**, *10*, 6287–6292.

(48) Loche, P.; Ayaz, C.; Schlaich, A.; Uematsu, Y.; Netz, R. R. Giant axial dielectric response in water-filled nanotubes and effective electrostatic ion-ion interactions from a tensorial dielectric model. *J. Phys. Chem. B* **2019**, *123*, 10850–10857.

(49) Motevaselian, M. H.; Aluru, N. R. Confinement-induced enhancement of parallel dielectric permittivity: Super permittivity under extreme confinement. *J. Phys. Chem. Lett.* **2020**, *11*, 10532–10537.

(50) Qi, C.; Zhu, Z.; Wang, C.; Zheng, Y. Anomalously low dielectric constant of ordered interfacial water. *J. Phys. Chem. Lett.* **2021**, *12*, 931–937.

(51) Friesen, A. D.; Matyushov, D. V. Local polarity excess at the interface of water with a nonpolar solute. *Chem. Phys. Lett.* **2011**, *511*, 256–261.

(52) Itoh, H.; Sakuma, H. Dielectric constant of water as a function of separation in a slab geometry: A molecular dynamics study. *J. Chem. Phys.* **2015**, *142*, 184703–11.

(53) Olivieri, J.-F.; Hynes, J. T.; Laage, D. Confined water's dielectric constant reduction is due to the surrounding low dielectric media and not to interfacial molecular ordering. *J. Phys. Chem. Lett.* **2021**, *12*, 4319–4326.

(54) Matyushov, D. V. In *Nonlinear Dielectric Spectroscopy*; Richert, R., Ed.; Springer: Cham, Switzerland, 2018; pp 1–34.

(55) Mondal, S.; Bagchi, B. Water layer at hydrophobic surface: Electrically dead but dynamically alive? *Nano Lett.* **2020**, *20*, 8959–8964.

(56) Fries, P. H.; Richardi, J.; Krienke, H. Dielectric and structural results for liquid acetonitrile, acetone and chloroform from the hypernetted chain molecular integral equation. *Mol. Phys.* **1997**, *90*, 841–853.

(57) Honig, B.; Nicholls, A. Classical electrostatics in biology and chemistry. *Science* **1995**, *268*, 1144–1149.

(58) Ashbaugh, H. S. Convergence of molecular and macroscopic continuum descriptions of ion hydration. *J. Phys. Chem. B* **2000**, *104*, 7235–7238.

(59) Doyle, C. C.; Shi, Y.; Beck, T. L. The importance of the water molecular quadrupole for estimating interfacial potential shifts acting on ions near the liquid–vapor interface. *J. Phys. Chem. B* **2019**, *123*, 3348–3358.

(60) Figueirido, F.; Del Buono, G. S.; Levy, R. M. On finite-size effects in computer simulations using the Ewald potential. *J. Chem. Phys.* **1995**, *103*, 6133–6142.

(61) Huston, S. E.; Rossky, P. J. Free energies of association for the sodium-dimethyl phosphate ion pair in aqueous solution. *J. Phys. Chem.* **1989**, *93*, 7888–7895.

(62) Pollock, E. L.; Alder, B. J. Frequency-dependent dielectric response in polar liquids. *Phys. Rev. Lett.* **1981**, *46*, 950–953.

(63) Chandra, A.; Bagchi, B. Collective excitations in a dense dipolar liquid: How important are dipolarons in the polarization relaxation of common dipolar liquids? *J. Chem. Phys.* **1998**, *92*, 6833.

(64) Jiménez-Ángeles, F.; Harmon, K. J.; Nguyen, T. D.; Fenter, P.; Olvera de la Cruz, M. Nonreciprocal interactions induced by water in confinement. *Phys. Rev. Res.* **2020**, *2*, 043244–18.

(65) Matyushov, D. V. Dielectric response of one-dimensional polar chains. *J. Chem. Phys.* **2007**, *127*, 054702.

(66) Köfinger, J.; Hummer, G.; Dellago, C. Macroscopically ordered water in nanopores. *Proc. Natl. Acad. Sci. USA* **2008**, *105*, 13218–13222.

(67) Loche, P.; Wolde-Kidan, A.; Schlaich, A.; Bonthuis, D. J.; Netz, R. R. Comment on "Hydrophobic surface enhances electrostatic interaction in water". *Phys. Rev. Lett.* **2019**, *123*, 049601.

(68) Sato, T.; Sasaki, T.; Ohnuki, J.; Umezawa, K.; Takano, M. Hydrophobic surface enhances electrostatic interaction in water. *Phys. Rev. Lett.* **2018**, *121*, 206002–5.

(69) Le, T. H. H.; Morita, A.; Tanaka, T. Refractive index of nanoconfined water reveals its anomalous physical properties. *Nanoscale Horiz.* **2020**, *5*, 1016–1024.

(70) Shen, Y. R. Sum frequency generation for vibrational spectroscopy: Applications to water interfaces and films of water and ice. *Solid State Comm.* **1998**, *108*, 399–406.

(71) Richmond, G. L. Molecular bonding and interactions at aqueous surfaces as probed by vibrational sum frequency spectroscopy. *Chem. Rev.* **2002**, *102*, 2693–2724.

(72) Shen, Y. R.; Ostroverkhov, V. Sum-frequency vibrational spectroscopy on water interfaces: Polar orientation of water molecules at interfaces. *Chem. Rev.* **2006**, *106*, 1140–1154.

(73) Velasco-Velez, J.-J.; Wu, C. H.; Pascal, T. A.; Wan, L. F.; Guo, J.; Prendergast, D.; Salmeron, M. Interfacial water. The structure of interfacial water on gold electrodes studied by x-ray absorption spectroscopy. *Science* **2014**, *346*, 831–834.

(74) Carpenter, A. P.; Tran, E.; Altman, R. M.; Richmond, G. L. Formation and surface-stabilizing contributions to bare nanoemulsions created with negligible surface charge. *Proc. Natl. Acad. Sci. USA* **2019**, *116*, 9214–9219.

(75) Singh, L. P.; Issenmann, B.; Caupin, F. Pressure dependence of viscosity in supercooled water and a unified approach for thermodynamic and dynamic anomalies of water. *Proc. Nat. Acad. Sci. USA* **2017**, *114*, 4312–4317.

(76) Teplukhin, A. V. Thermodynamic and structural characteristics of SPC/E water at 290 K and under high pressure. *J. Struct. Chem.* **2019**, *60*, 1590–1598.

(77) Zhao, X.; Ong, S.; Wang, H.; Eisenthal, K. B. New method for determination of surface pK_a using second harmonic generation. *Chem. Phys. Lett.* **1993**, *214*, 203–207.

TOC Graphic